Desalination and Water Treatment
www.deswater.com

doi:10.5004/dwt.2017.0468

69 (2017) 210–216
March

Pressure drop of steam condensation flow in vacuum horizontal tube for LT-MEE desalination plant

Yaoxuan Wang, Xingsen Mu, Shengqiang Shen*, Wenjie Zhang

Key Laboratory of Liaoning Province for Desalination, Dalian University of Technology, Dalian, China, Tel. +86 15041131789; email: wangyaoxuan@mail.dlut.edu.cn (Y. Wang), Tel. +86 13591366001; email: magicruby@gmail.com (X. Mu), Tel. +86 411 84708464; Fax: +86 411 84707963; email: zzbshen@dlut.edu.cn (S. Shen), Tel. +86 18340878705; email: zwj3202@126.com (W. Zhang)

Received 26 April 2016; Accepted 22 June 2016

ABSTRACT

An experimental system was built up to measure the pressure drop of steam condensation flow in vacuum horizontal aluminium brass tubes, whose inner diameter is 18 mm and length is 2 m. The experiments were carried out at the saturation temperatures varying from 50°C to 70°C with mass flow rate changing between 2 and 11 kg/(m²·s). The temperature differences between steam and cooling water are 3°C, 5°C and 7°C, respectively. Pressure drop decreases along flow direction. Pressure drop increases with mass flow rate and vapor quality, decreases with saturation temperature. Temperature difference has less effect on pressure drop. The saturation temperature depression rises at first and remains at a constant level later with the increase of flow direction. Saturation temperature depression increases with mass flow rate and decreases with temperature difference and saturation temperature. Based on the experimental data, a correlation was proposed for calculating pressure drop of steam condensation flow in vacuum horizontal tube.

Keywords: Pressure drop; Steam condensation; Horizontal tube; Desalination

1. Introduction

Population growth, urbanization, migration and industrialization, along with increases in production and consumption, have generated ever-increasing demands for freshwater resources [1]. Low-temperature multi-effect evaporation (LT-MEE) technique has the benefits of high thermal efficiency, insensitivity to the quality of the feed and stable operation. So it is widely used for desalination process to relief the crisis of water resource and the installed capacity accounts for more than 8% of the total installed capacity of desalination in the world [2]. In this technique, steam condensates in the horizontal tube, which provides heat source for seawater evaporating out the tube. The pressure drop of steam condensation flow in vacuum horizontal tube is an important parameter which influences both flow and heat transfer in the system.

The MEE desalination system has been studied extensively, however the effect of steam condensation pressure drop has received less attention. The MEE system model proposed by Darwish and Abdulrahim [3] is one of the most cited model, which ignores the pressure drop of steam condensation. Other scholars [4–9] simulated and optimized the MEE units with the assumption that pressure drop of steam condensation can be neglected. Kouhikamali et al. [10] investigated the pressure drop in the heat exchangers of multi-effect evaporation with thermal vapor compression system and showed that condensation pressure drop in the tube has most influence on the system performance among all different kinds of pressure losses. Considering condensation pressure drop in tube increases the specific heat transfer surface area by about 7% than neglecting it.

*Corresponding author.

Presented at the EDS conference on Desalination for the Environment: Clean Water and Energy, Rome, Italy, 22–26 May 2016.

Liu et al. [11] experimentally studied the shell-side two-phase pressure drop on falling film evaporation in a rotated square bundle in LT-MEE desalination plant. Zhou et al. [12] analyzed the distribution of various thermodynamic losses which include flow resistances in the whole LT-MEE desalination plant.

Some models [13–15] include the condensation pressure drop, which is calculated by the following equations. The pressure drop Δp is the sum of static pressure drop Δp_{static}, the momentum pressure drop Δp_{mom} and the frictional pressure drop Δp_{frict}.

$$\Delta p = \Delta p_{static} + \Delta p_{mom} + \Delta p_{frict} \tag{1}$$

The static pressure drop Δp_{static} is zero for horizontal tube, and the momentum pressure drop Δp_{mom} is given by:

$$\Delta p_{mom} = G^2 \left\{ \left[\frac{(1-x)^2}{\rho_l(1-\alpha)} + \frac{x^2}{\rho_v \alpha} \right]_{out} - \left[\frac{(1-x)^2}{\rho_l(1-\alpha)} + \frac{x^2}{\rho_v \alpha} \right]_{in} \right\} \tag{2}$$

where, the void fraction is calculated by Zivi [16] correlation. The frictional pressure drop Δp_{frict} is calculated by Friedel [17] correlation:

$$\Delta p_{frict} = \Delta p_l \phi_{lo}^2 \tag{3}$$

Zivi correlation was derived by the theory of minimum entropy production which is suitable for steady state annular flow. Friedel correlation is a function of property ratios, Froude number and Weber number, based on experiments with R12, air-water and air-oil. As the steam condensation flow in tube in the MEE desalination system is normally a stratified flow, with the characteristic of high vacuum and low mass flow rate. The Zivi correlation and Friedel correlation are not completely suitable for this condition.

Pressure drop of two phase flow is important not only in MEE desalination, but also in different industrial applications, such as refrigeration, air condition system and pipeline network system. A large number of experimental studies were carried out, but most of the working fluids are refrigerants, few of them are steam at high pressure or atmospheric pressure. Pressure drop of steam in vacuum condition are rarely reported in former literatures. In this paper, this issue will be studied experimentally.

2. Experimental apparatus

The major objecive of the experiment is to measure the pressure drop of steam condensation flow. As shown in Fig. 1, the experimental apparatus contain steam loop, cooling water loop and the data acquisition system. Steam is provided by an evaporator with 12 kW electric power. Demister is installed at the outlet of the evaporator to ensure that the vapor quality is near 1. Then, steam flows through five identical test sections, where all or part of steam condenses into water. Subsequently, water is separated from the steam-water mixture and stays in the separator which is connected to the last test section. Finally, uncondensed steam flows into two condensers and condenses into water completely by cooling water. Liquid level meters on the separator and condensers are uesd to measure the mass flow rates of steam and condensation water. A vacuum pump connected to the second condenser enables the system to achieve and maintain vacuum state. The total length of test tube is 10m to simulate the two-phase flow in the actual LT-MEE desalination plant. The test tube is divided into five segments in order to reduce the increment of cooling water temperature. A cooling water tank and a water pump are used to provide cooling water at constant temperature to five test sections, respectively.

The test sections are double-pipe heat exchangers, shown in Fig. 2. Steam condensates in the inner tube while cooling water flows countercuttently through the annulus. The inner tube is made of aluminium brass with 18 mm in inner diameter, 0.5 mm in thickness and 2 m in length. The outer tube is made of stainless steel with 35 mm inner diameter.

Cooling water temperatures are measured by T-type thermocouples at the inlet and outlet of cooling water in each test section. Thermocouples are also welded on the test tube to measure the tube wall temperature. All the thermocouples

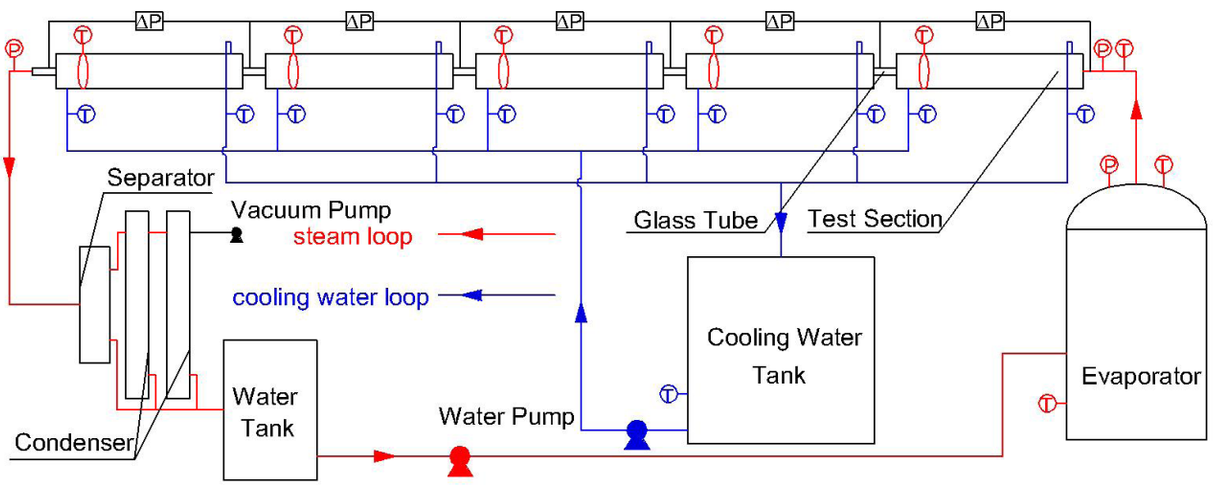

Fig. 1. Schematic diagram of experimental apparatus.

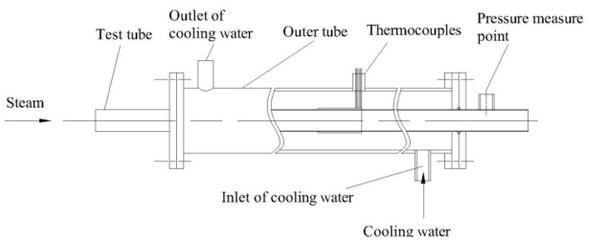

Fig. 2. Geometry of the test section.

are calibrated by thermostatic waterbath with an accuracy of 0.1°C. The pressure measure point is 350 mm from the end of test tube. Differential pressure transducers with an accuracy of 0.1% within its full span are installed between two adjacent pressure measure points, so the pressure drop of steam condensation flow in each test section can be measured. Pressure transducers with a precision of ± 28 Pa are installed at the inlet and outlet of the test tube and the evaporator to monitor the vacuum state of the system. The records of differential pressure transducers and pressure transducers are instantaneous values of an interval of 3 s. In each experimental condition, 200 data are recorded and the average of whose values are calculated by a computer equipped with a National Instruments SCXI data acquisition system.

The experimental conditions and actual operation of LT-MEE desalination system parameters are quite similar. The saturation temperature in the actual plant is generally lower than 70°C for the purpose of preventing fouling. The experiments were carried out at the saturation temperature varying from 50°C to 70°C and mass flow rate changing between 2 and 11 kg/(m²·s). The temperature differences between steam and cooling water are 3°C, 5°C and 7°C at the end of test section, respectively.

3. Data processing

Heat transfer rate Q in each test section is calculated by the following formula:

$$Q = m_c c_p \left(T_{c,out} - T_{c,in}\right) \tag{4}$$

where, m_c is the mass flow rate of cooling water, and c_p is the constant-pressure specific heat of water. $T_{c,in}$ and $T_{c,out}$ are the cooling water temperature at the inlet and outlet of test section, respectively. The vapor quality at the inlet of the first test tube is 1. The vapor quality at the inlet and outlet of test tube i are calculated as the following:

$$x_{i,in} = 1 - \frac{\sum_{1}^{i-1} Q_i}{m_s \gamma} \quad x_{i,out} = 1 - \frac{\sum_{1}^{i} Q_i}{m_s \gamma} \tag{5}$$

where m_s is the mass flow rate of steam, γ is the latent heat. So, the average vapor quality in test tube i can be calculated as:

$$x_i = \frac{1}{2}\left(x_{i,in} + x_{i,out}\right) \tag{6}$$

The saturation temperature depression ΔT_d is defined by the following formula:

$$\Delta T_d = T_{s,in} - T_s \tag{7}$$

where T_s is the steam temperature and $T_{s,in}$ is the steam temperature at the inlet of the test section.

4. Experimental data and discussion

4.1. Pressure drop distribution along flow direction

The pressure drop distribution along flow direction at different mass flow rates are shown in Fig. 3, when the saturation temperature is 60°C at the end of test tube. The pressure drop shows a downward trend along flow direction. The pressure drop is maximum in the first test tube but relatively small in the other four test tubes. With the condensation process, steam velocity decreases significantly, and the tube inner wall is covered by liquid film. These reasons result in reduced friction, so the pressure drop declines. The downward trend becomes rapid when the mass flow rate increases. The pressure drop changes from 124 Pa/m to about 0 Pa/m at G = 5.5 kg/(m²·s). In comparison, it changes from 531 to 72P a/m at G = 9.6 kg/(m²·s).

4.2. Effects of mass flow rate and vapor quality

Fig. 4 shows the effects of mass flow rate and vapor quality on pressure drop when the saturation temperature is 60°C at the end of test tube. The pressure drop rises as the mass flow rate and vapor quality increase. Pressure drop increases dramatically at high vapor quality or high mass flow rate. Increasing the mass flow rate and vapor quality lead to the increase of steam velocity obviously, so the pressure drop increases rapidly. The pressure drop grows 459 Pa/m at x = 0.9 when the mass flow rate changes from 6.3 to 9.6 kg/(m²·s). At the same time, it increases only 228 Pa/m at x = 0.3.

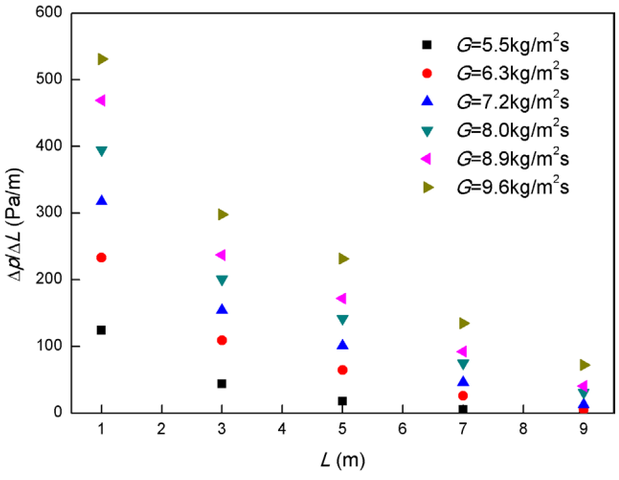

Fig. 3. Pressure drop distribution along flow direction.

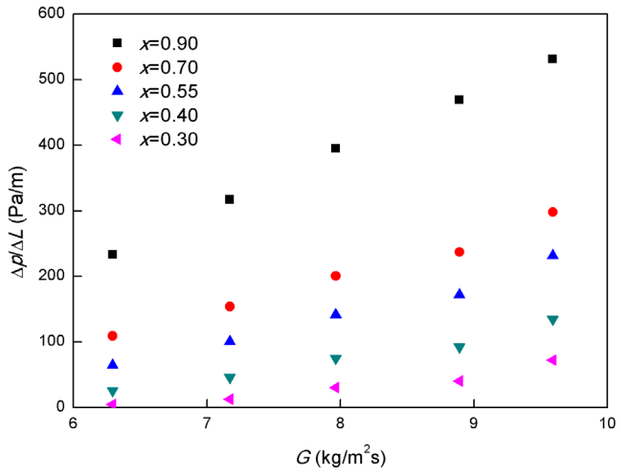

Fig. 4. Effect of mass flow rate and vapor quality on pressure drop.

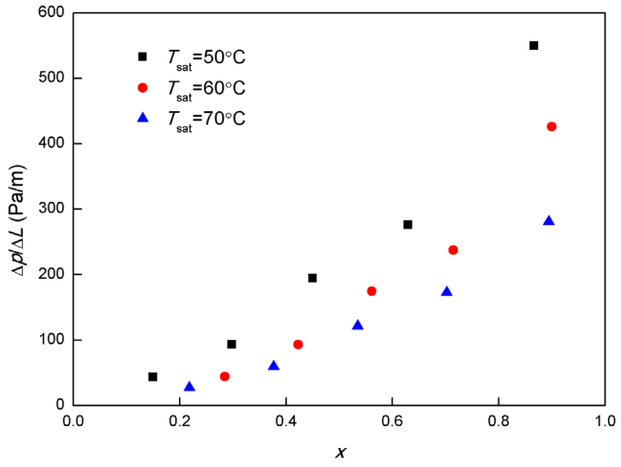

Fig. 5. Effect of saturation temperature on pressure drop.

4.3. Effect of saturation temperature

Saturation temperature has a great influence on the physical properties of steam and water, thereby affecting the pressure drop. When the mass flow rate is constant, steam velocity decreases as the saturation temperature increases, due to the steam density increases with temperature. Liquid film formed on the inner tube wall with condensation process. The dynamic viscosity plays an important role in friction between steam and liquid film. When saturation temperature increases from 50°C to 70°C, steam dynamic viscosity increases 8% and water dynamic viscosity decreases 26%. The dynamic viscosity of water is about 50 times of steam. Low steam velocity and low water dynamic viscosity lead to the decrease of friction generated by steam flow obviously. So the pressure drop declines with the rising saturation temperature, as shown in Fig. 5. The saturation temperature plays a more important role on pressure drop when the vapor quality is high. The pressure drop tends to be the same at different saturation temperatures when the vapor quality is low. The difference of pressure drop varying from T_{sat} = 50°C to T_{sat} = 60°C at the same vapor quality is greater than what is varying from T_{sat} = 60°C to T_{sat} = 70°C, which is due to the varying gradient of the physical properties with temperature.

4.4. Effect of temperature difference

The effect of temperature difference on pressure drop is shown in Fig. 6 when the mass flow rate is 8.5 kg/(m²·s) and the saturation temperature is 60°C at the end of test tube. The temperature differences between steam and cooling water at the end of the test tube are 3°C, 5°C and 7°C, respectively. The experimental data at different temperature difference are almost in the same curve. So temperature difference has less effect on pressure drop. Large temperature difference represents high heat transfer rate which leads to decrease of vapor quality and pressure drop in the test section at same time.

4.5. Saturation temperature depression distribution along flow direction

There is a one-to-one correspondence between pressure and saturation temperature. The pressure and saturation temperature reduce at same time along the flow direction because of flow resistance. Fig. 7 shows the saturation temperature depression distribution along flow direction at different mass flow rates when the saturation temperature is 50°C and temperature differences are 3°C and 7°C, respectively. The pressure decrement increases steadily with flow direction before steam condensates into water completely, and then pressure decrement is almost 0 Pa. Hence, the saturation temperature depression rises at first and remains constant later with the increase of flow direction. The saturation temperature depression and the slope of saturation temperature depression variarion both increase with the rising of mass flow rate, because large mass flow rate results in large pressure drop. The distance of saturation temperature depression increase is longer when the mass flow rate is higher. In particular cases, saturation temperature depression rises in the whole test tube and does not convert to stable, for example, G = 8.1 kg/(m²·s) and $\Delta T_{s,c}$ = 3°C. Fig. 7 also

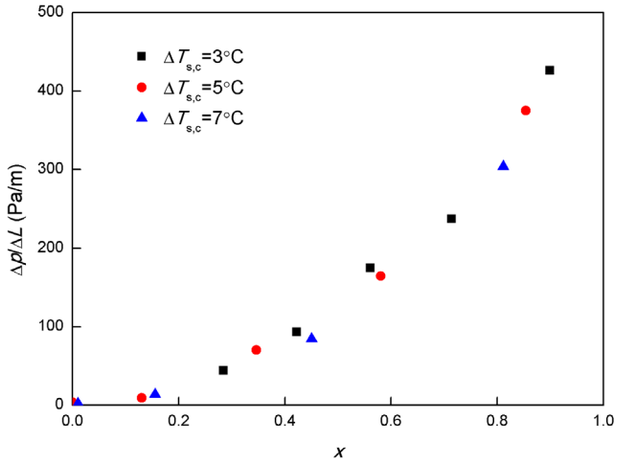

Fig. 6. Effect of temperature difference on pressure drop.

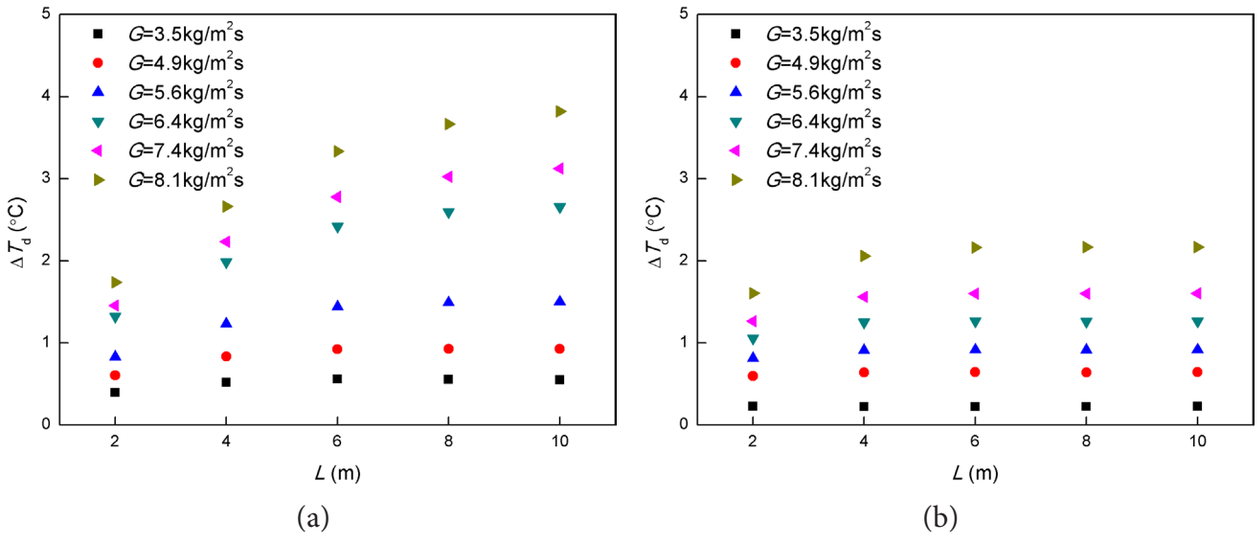

Fig. 7. Saturation temperature depression distribution along flow direction. (1) $\Delta T_{s,c}$=3°C (2) $\Delta T_{s,c}$=7°C.

shows that saturation temperature depression is smaller when the temperature difference is larger. Large temperature difference represents high heat transfer rate, so steam condensates into water completely in a relative short length in the tube when the mass flow rate is constant. Short length means small total pressure decrement because the pressure drop has less relationship with temperature difference.

4.6. Effect of saturation temperature on saturation temperature depression

The relationship between pressure variation and saturation temperature when saturation temperature changes 0.1°C presents a power function, as shown in Fig. 8. The pressure variation is only 61 Pa when the saturation temperature is 50°C, and grows to 92 and 135 Pa when the saturation temperatures are 60°C and 70°C. So the effect of flow resistance is more significant on saturation temperature when the saturation temperature is lower.

Fig. 9 shows the effect of saturation temperature on saturation temperature depression when the mass flow rate is 8.5 kg/(m²·s). It can be seen from the above analysis that the pressure drop declines with the increase of saturation temperature. So the saturation temperature depression falls sharply with the increase of saturation temperature. For example, saturation temperature depression changes from 3.82°C to 1.06°C when the saturation temperature increases from 50°C to 70°C at the location of 10 m.

4.7. Compare with Friedel correlation

Friedel [17] correlation was widely used to calculate the pressure drop in MEE desalination. The two phase friction multiplier is calculared by the following equations:

$$\phi_{lo}^2 = (1-x)^2 + x^2 \frac{\rho_l f_{so}}{\rho_s f_{lo}} + \frac{3.24 x^{0.78} (1-x)^{0.224} H}{Fr_{tp}^{0.045} We_{tp}^{0.035}} \quad (8)$$

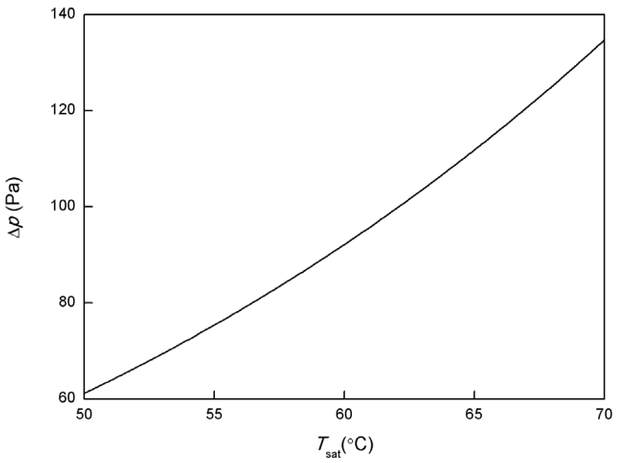

Fig. 8. The pressure variation vs. saturation temperature when saturation temperature changes 0.1°C.

$$H = \left(\frac{\rho_l}{\rho_s}\right)^{0.91} \left(\frac{\mu_s}{\mu_l}\right)^{0.19} \left(1 - \frac{\mu_s}{\mu_l}\right)^{0.7} \quad (9)$$

The comparison between experimental data of pressure drop and predicted data using Friedel correlation is shown in Fig. 10. It can be seen from the figure that the pressure drop is significantly undervalued when the pressure drop is high. So the Friedel correlation is not suitable for LT-MEE desalination system.

4.8. New correlation for pressure drop in tube

The existing pressure drop correlations were based on experimental data of refrigerants or steam at high pressure or atmospheric pressure. The experimental conditions which the existing correlations based on, are different from

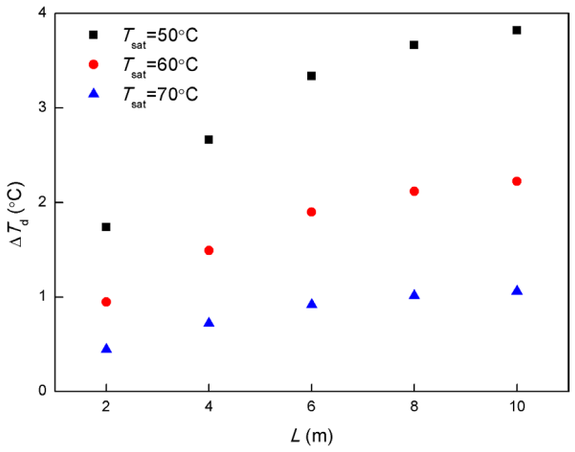

Fig. 9. Effect of saturation temperature on saturation temperature depression.

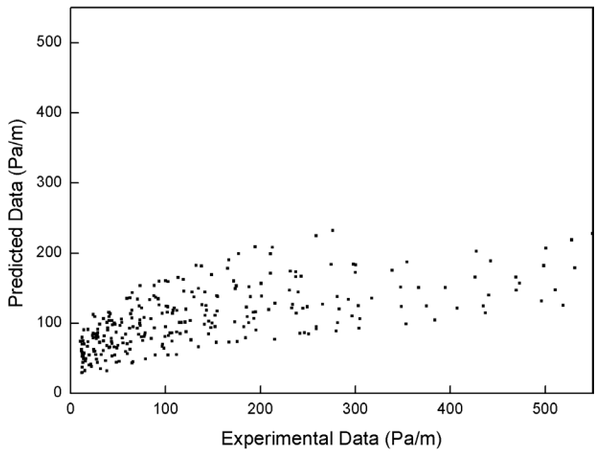

Fig. 10. Comparison of experimental pressure drop and Friedel correlation.

the operation condition of LT-MEE desalination system. The database for new correlation is the experimental data excluding the portion of less than 10 Pa/m at the saturation temperature varying from 50°C to 70°C, vapor quality varying from 0 to 1 and mass flow rate changing between 2 and 11 kg/(m²·s). A new correlation is developed based on 260 data points. As mentioned above, the main factors that influence pressure drop are mass flow rate, vapor quality and physical properties. The new correlation has the following form:

$$\frac{\Delta p}{\Delta L} = a\frac{G^2}{2d\rho_{tp}}x^b\left(\frac{\mu_l}{\mu_s}\right)^c \tag{10}$$

where a, b and c are undetermined coefficients, and ρ_{tp} is the two-phase density, its form is as follow:

$$\frac{1}{\rho_{tp}} = \frac{1-x}{\rho_l} + \frac{x}{\rho_s} \tag{11}$$

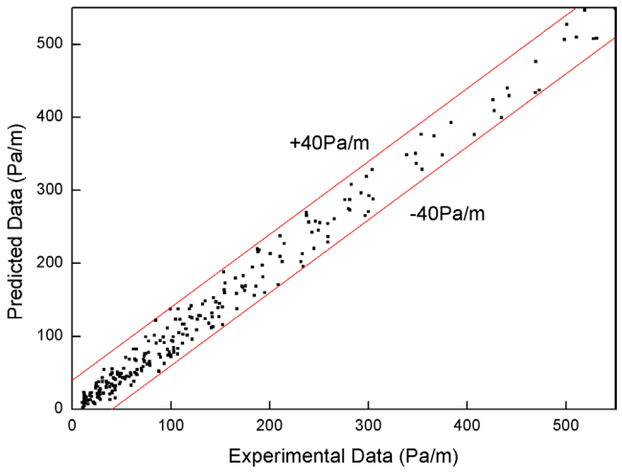

Fig 11. Comparison of experimental and predicted pressure drop.

Based on the principle of least square method, use multiple linear regression to compute the undetermined coefficients. The new correlation is shown as follow:

$$\frac{\Delta p}{\Delta L} = 0.03\frac{G^2}{2d\rho_{tp}}x^{1.03}\left(\frac{\mu_l}{\mu_s}\right)^{0.02} \tag{12}$$

Fig. 11 shows a comparison between the experimental data of pressure drop and predicted data using the new correlation. The result shows that the deviations between experimental data and calculated values are less than 40Pa/m.

5. Conclusion

Pressure drop of steam condensation flow in vacuum horizontal tube were investigated experimentally. Some conclusions can be summarized as following.

- Pressure drop decreases along flow direction. Pressure drop increases with mass flow rate and vapor quality, decreases with saturation temperature. Temperature difference has less effect on pressure drop.
- The saturation temperature depression rises at first and remains at a constant level later with the increase of flow direction. Saturation temperature depression increases with mass flow rate and decreases with temperature difference and saturation temperature.
- Based on experimental data, a new correlation was proposed for calculating pressure drop of steam condensation flow in vacuum horizontal tube. The deviations between experimental data and calculated values are less than 40Pa/m.

Acknowledgment

The research is supported by the Key Project of National Science Foundation of China (No.51336001) and Science and Technology Support Program (2014BAB09B00).

Symbols

c_p	—	Constant pressure specific heat, kJ/(kg°C)
d	—	Diameter, m
f	—	Friction factor
Fr	—	FROUDE number
G	—	Mass flow rate, kg/(m²·s)
m	—	Mass flow rate, kg/s
p	—	Pressure, Pa
L	—	Length, m
Q	—	Heat transfer rate, kW
R_e	—	Reynolds number
T	—	Temperature, °C
We	—	Webb number
x	—	Vapor quality

Greek

Δ	—	Difference
α	—	Void fraction
γ	—	Latent heat, kJ/kg
μ	—	Dynamic viscosity, Pa·s
ρ	—	Density, kg/m³
φ²	—	Two phase friction multiplier

Subscripts

c	—	Cooling water
d	—	Depression
frict	—	Frictional
i	—	Ordinal number
in	—	Inlet
l	—	Liquid
lo	—	Liquid only
mom	—	Momentum
out	—	Outlet
s	—	Steam
so	—	Steam only
sat	—	Saturation
static	—	Static
tp	—	Two-phase

References

[1] UNESCO, The United Nations World Water Development Report 2015: Water for a Sustainable World, 2015.
[2] N. Ghaffour, T.M. Missimer, G.L. Amy, Technical review and evaluation of the economics of water desalination: current and future challenges for better water supply sustainability, Desalination, 309 (2013) 197–207.
[3] M. Darwish, H.K. Abdulrahim, Feed water arrangements in a multi-effect desalting system, Desalination, 228 (2008) 30–54.
[4] N.H. Aly, A.K. El-Figi, Thermal performance of seawater desalination systems, Desalination, 158 (2003) 127–142.
[5] P. Druetta, P. Aguirre, S. Mussati, Optimization of multi-effect evaporation desalination plants, Desalination, 311 (2013) 1–15.
[6] R. Kamali, A. Abbassi, S.S. Vanini, A simulation model and parametric study of MED–TVC process, Desalination, 235 (2009) 340–351.
[7] M. Kazemian, A. Behzadmehr, S. Sarvari, Thermodynamic optimization of multi-effect desalination plant using the DoE method, Desalination, 257 (2010) 195–205.
[8] M. Khademi, M. Rahimpour, A. Jahanmiri, Simulation and optimization of a six-effect evaporator in a desalination process, Chem. Eng. Process. Process Intensif., 48 (2009) 339–347.
[9] P. Palenzuela, A.S. Hassan, G. Zaragoza, D.-C. Alarcón-Padilla, Steady state model for multi-effect distillation case study: plataforma Solar de Almería MED pilot plant, Desalination, 337 (2014) 31–42.
[10] R. Kouhikamali, A.S. Kojidi, M. Asgari, F. Alamolhoda, The effect of condensation and evaporation pressure drop on specific heat transfer surface area and energy consumption in MED–TVC plants, Desal. Wat. Treat., 46 (2012) 68–74.
[11] H. Liu, S. Shen, L. Gong, S. Chen, Shell-side two-phase pressure drop and evaporation temperature drop on falling film evaporation in a rotated square bundle, Appl. Therm. Eng., 69 (2014) 214–220.
[12] S. Zhou, Y. Guo, X. Mu, S. Shen, Effect of design parameters on thermodynamic losses of the heat transfer process in LT-MEE desalination plant, Desalination, 375 (2015) 40–47.
[13] M. Ameri, S.S. Mohammadi, M. Hosseini, M. Seifi, Effect of design parameters on multi-effect desalinationsystem specifications, Desalination, 245 (2009) 266–283.
[14] H.T. El-Dessouky, H.M. Ettouney, F. Mandani, Performance of parallel feed multiple effect evaporation system for seawater desalination, Appl. Therm. Eng., 20 (2000) 1679–1706.
[15] H. Hou, Q. Bi, X. Zhang, Numerical simulation and performance analysis of horizontal-tube falling-film evaporators in seawater desalination, Int. Commun. Heat. Mass., 39 (2012) 46–51.
[16] S. Zivi, Estimation of steady-state steam void-fraction by means of the principle of minimum entropy production, J. Heat. Transfer, 86 (1964) 247.
[17] L. Friedel, Improved Friction Pressure Drop Correlations for Horizontal and Vertical Two-phase Pipe Flow, European Two-phase Flow Group Meeting, Paper E, Ispra, Italy, June 1979.